

Measurement of two-halo neutron transfer reaction $p(^{11}\text{Li}, ^9\text{Li})t$ at 3A MeV

I. Tanihata,* M. Alcorta,† D. Bandyopadhyay, R. Bieri, L. Buchmann, B. Davids, N. Galinski, D. Howell, W. Mills, R. Openshaw, E. Padilla-Rodal, G. Ruprecht, G. Sheffer, A. C. Shotter, S. Mythili, M. Trinczek, and P. Walden
TRIUMF, 4004 Wesbrook Mall, Vancouver, BC, V6T 2A3, Canada

H. Savajols, T. Roger, M. Caamano, W. Mittig,‡ and P. Roussel-Chomaz
GANIL, Bd Henri Becquerel, BP 55027, 14076 Caen Cedex 05, France

R. Kanungo and A. Gallant
Saint Mary's University, 923 Robie St., Halifax, Nova Scotia B3H 3C3, Canada

M. Notani and G. Savard
ANL, 9700 S. Cass Ave., Argonne, IL 60439, USA

I. J. Thompson
LLNL, L-414, P.O. Box 808, Livermore CA 94551, USA
(Dated: (received on))

The $p(^{11}\text{Li}, ^9\text{Li})t$ reaction has been studied for the first time at an incident energy of 3A MeV delivered by the new ISAC-2 facility at TRIUMF. An active target detector MAYA, build at GANIL, was used for the measurement. The differential cross sections have been determined for transitions to the ^9Li ground and the first excited states in a wide range of scattering angles. Multistep transfer calculations using different ^{11}Li model wave functions, shows that wave functions with strong correlations between the halo neutrons are the most successful in reproducing the observation.

PACS numbers: 25.40.Hs, 27.20.+n, 24.10.Eq, 21.90.+f

The neutron-rich Li isotope ^{11}Li has the most pronounced two-neutron halo. Presently the most important question about the halo structure concerns the nature of the interaction and correlation between the two halo neutrons. In a halo, the correlation may be different from that of a pair of neutrons in normal nuclei for several reasons. Halo neutrons are very weakly bound and, therefore, the effect of the continuum becomes important. The wave function of the halo neutrons has an extremely small overlap with that of the protons and, thus, may experience interactions much different from those of neutrons in normal nuclei. The density of halo neutrons is very low compared with normal nuclear density and, thus, may give rise to quite different correlations from that in stable or near-stable nuclei. So far, there have been several experimental attempts to elucidate the nature of these correlations between the halo neutrons in ^{11}Li . For example, measurements of neutrons and ^9Li from the fragmentation of ^{11}Li have been used to determine the momentum correlation between two halo neutrons [1]. However, the contribution of the ^{10}Li resonance, which decays to $^9\text{Li}+n$ immediately, made it difficult to reach definitive conclusions. Later, Zinser et al. [2] studied high-energy stripping reactions of ^{11}Li and ^{11}Be to ^{10}Li , and the analyses of the momentum distributions suggests the necessity of considerable mixing of $(1s_{1/2})^2$ and $(0p_{1/2})^2$ configurations in the ground state of ^{11}Li . The importance of the s-wave contribution is also seen in Coulomb dissociation measurements [3, 4]. Determinations of such amplitudes have also been attempted from data associated with the beta-decay of ^{11}Li ; however, no definite conclusions could be reached.

A recent measurement of the charge radius of ^{11}Li and ^9Li [5], when combined with the matter radii of ^{11}Li and ^9Li [6], provides unique information concerning the two-neutron distribution. The root-mean-square(rms) distance between two halo neutrons $\langle r_{n-n}^2 \rangle^{1/2}$, as well as the distance between the two-neutron center-of-mass and the center of the core $\langle r_{c-2n}^2 \rangle^{1/2}$, can be evaluated under two assumptions: a) that ^{11}Li consists of a ^9Li core plus two halo neutrons and b) that there is no angular correlation between the position vector connecting the two-halo neutrons and the position vector connecting the center of mass of the two-neutrons to the center of the core. Taking these assumptions into account, and using experimental data from references [5, 6], we obtain $\langle r_{n-n}^2 \rangle^{1/2} = 7.52 \pm 1.72$ fm and $\langle r_{c-2n}^2 \rangle^{1/2} = 6.15 \pm 0.52$ fm. This shows that the average opening angle of the two-halo neutrons, relative to the core centre, is about 60 degrees. Similar analysis can be made for ^6He , if again it is assumed: $^6\text{He} \rightarrow ^4\text{He} + n + n$. From this, and using measured matter and charge radii of ^4He [6, 7], we obtain $\langle r_{n-n}^2 \rangle^{1/2} = 3.91 \pm 0.28$ fm, and $\langle r_{c-2n}^2 \rangle^{1/2} = 3.84 \pm 0.06$ fm. The average opening angle in this case is 54 degrees.

In ^6He case the wave function of the halo is known better than that of ^{11}Li because it is mainly of a $p_{3/2}$ character. From three-body calculations two separate components (di-neutron and cigar shape) contribute almost equally to

the halo structure [8]. Experimental observations for the two-neutron transfer reaction, ${}^6\text{He} + {}^4\text{He} \rightarrow {}^4\text{He} + {}^6\text{He}$, (backward elastic scattering included) yields results consistent with such theoretical calculations [9]. Although it seems that the relation between $\langle r_{n-n}^2 \rangle^{1/2}$ and $\langle r_{c-2n}^2 \rangle^{1/2}$ is similar between ${}^{11}\text{Li}$ and ${}^6\text{He}$, differences in the structure of the wave functions are expected because of the complexity of the ${}^{11}\text{Li}$ wave function, namely a mixing of two different orbitals ($1s_{1/2}$ and $0p_{1/2}$). The mixing amplitude of these waves is an important factor that determines the binding and the halo structure in ${}^{11}\text{Li}$.

The newly constructed ISAC-2 accelerator at TRIUMF now provides the highest intensity beam of low-energy ${}^{11}\text{Li}$ up to 55 MeV. This beam enabled the measurement of the two-neutron transfer reaction of ${}^{11}\text{Li}$ for the first time. The reaction Q-value of ${}^{11}\text{Li}(p,t){}^9\text{Li}$ is very large (8.2 MeV) and, thus, the reaction channel is open at such low energies. The beam energy used in this experiment (33 MeV) is not as high as usually used in studies of direct reactions, nevertheless due to the low separation energy of the two halo neutrons (~ 400 keV compared with about 10 MeV in stable nuclei) and low Coulomb barrier (~ 0.5 MeV) the reaction is expected to be mainly direct. Momentum matching is also good at this low energy because of the small internal momentum of the halo neutrons.

The beam of ${}^{11}\text{Li}$ was accelerated to energy of 36.9 MeV. Beam intensity on the target was about 2500 pps on average, and about 5000 pps at maximum. Measurement of the transfer reaction was made possible at this low beam intensity through the use of the MAYA active target detector brought to TRIUMF from GANIL. MAYA has a target-gas detection volume (28 cm long in the beam direction, 25 cm wide, and 20 cm high) for three-dimensional tracking of charged particles, and a detector telescope array at the end of the chamber. Each detector telescope consisted of a $700 \mu\text{m}$ thick Si detector and a 1 cm thick CsI scintillation counter of $5 \times 5 \text{ cm}^2$. The array consists of twenty sets of telescopes. MAYA was operated with isobutane gas first at a gas pressure of 137.4 mbar and then at 91.6 mbar. These two different pressure settings were used to cross check the validity of the analysis by changing the drift speed of ionized electrons and by changing the energy loss density. The coverage of center of mass angles was also different under these pressures - as will be discussed later. Reaction events were identified by a coincidence between a parallel plate avalanche chamber (PPAC), which is placed just upstream of MAYA, and the Si array. ${}^{11}\text{Li}$ ions that did not undergo a reaction were stopped in the blocking material just before the Si array. Details of MAYA can be found in Ref.[10].

The two-neutron transfer reaction $p({}^{11}\text{Li}, {}^9\text{Li})t$ was identified by two methods depending on the scattering angles. For forward scattering in the c.m., ${}^9\text{Li}$ ions in the laboratory frame are emitted at small angles and have sufficient energies to traverse the gas and hit the Si array, and so ${}^9\text{Li}$ ions were identified by the $\Delta E - E$ method. The ΔE signal was obtained from the last 5 cm of the MAYA gas detector. Tritons emitted near 90 degrees have low energies so that they stop within the gas detector and thus provide total energy signals. However tritons emitted in smaller angles, but larger than the angle covered by the Si array, punch through the gas volume and therefore only scattering angles and partial energy losses in the chamber could be measured. The major background for such events came from the ${}^{11}\text{Li} + p \rightarrow {}^{10}\text{Li} + d \rightarrow {}^9\text{Li} + n + d$ reaction. Fortunately, the kinematical locus in a two-dimensional plot between emission angles of ${}^9\text{Li}$ and light particles, $[\theta(\text{Li}) - \theta(\text{light})]$, of the (p,d) reaction is well separated from the punch through (p,t) events.

For large angle scattering in the c.m., tritons were detected by the Si and CsI detectors and identified clearly by the $\Delta E - E$ technique. Under this condition, ${}^9\text{Li}$ stops inside the gas detector volume and thus the total energy, the range, and the scattering angle were determined. Lithium ions can easily be identified from their energy loss along the track, but identification of the isotope mass number is more difficult. The largest background events are due to scattered ${}^{11}\text{Li}$ with accidental coincidence that have higher energies and will hit the Si array. So rejection of such ${}^{11}\text{Li}$ events was easily accomplished. Use again was made of a $\theta(\text{Li}) - \theta(\text{light})$ correlation plot for final identification of the (p,t) reaction. To remove other sources of background, additional selections were applied. For forward angle events, important correlations for these selections were: $E(\text{Li}) - \theta(\text{Li})$, $E(\text{Li}) - \theta(\text{H})$, and $Q_c(\text{H}) - \theta(\text{H})$, where E is the energy of a particle determined by Si array and Q_c is the total charge collected in the gas detection volume. The last correlation was effective for removing deuterons. For the large angle events, the most important correlation was $E(t) - \theta(\text{heavy})$; here “heavy” means $Z = 3$ particles detected in the gas detector volume.

Figure 1(a) shows $\theta(\text{heavy})$ vs. $\theta(\text{light})$ scatter plot after those selections. Two clear kinematic loci are seen. The reaction Q-value spectra calculated from those angles are shown in the panel (b). The spectra show the transitions to the ground state of ${}^9\text{Li}$ as well as the transition to the first excited state ${}^9\text{Li}$ (2.69 MeV). Mixing of ground state transition into the first excited state spectrum is seen in the plot but, can easily be removed by the selection of the Q values. The tracking efficiency was determined by comparing the number of identified particles (by the $\Delta E - E$ method) and the number of tracks that hit an array detector at consistent position; this comparison was undertaken separately for Li and triton ions. The geometrical efficiency was estimated by a Monte-Carlo simulation that includes detector geometries and energy losses of the charged particles in the gas.

The number of incident ${}^{11}\text{Li}$ ions was determined by counting the incident ions both by the PPAC and signals from

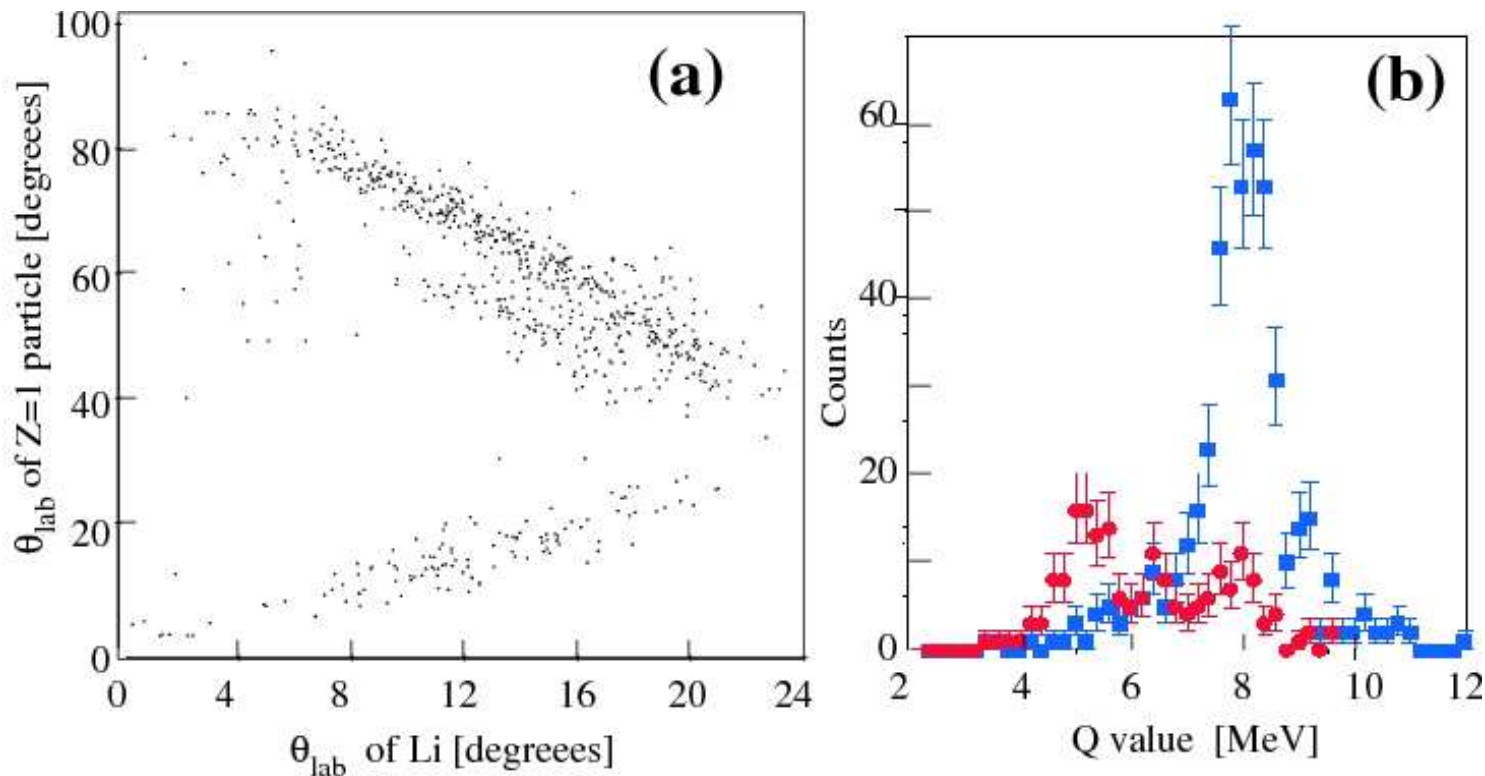


Fig. 1 (a) $\theta(\text{Li})-\theta(\text{H})$ plot. Loci of (p,t) reactions are clearly seen. (b) Q-value histograms of (p,t) reactions. Blue points show the spectrum for ${}^9\text{Li}$ ground state transition and Red points are for the first excited state of ${}^9\text{Li}$.

FIG. 1: (a) $\theta(\text{Li}) - \theta(\text{H})$ plot. Loci of (p,t) reactions are clearly seen. (b) Q-value histograms of (p,t) reactions. Blue points show the spectrum for ${}^9\text{Li}$ ground state transition and Red points are for the first excited state of ${}^9\text{Li}$.

the first 7 cm of the gas detector. The position, direction, and energy loss along the track of an incident particle were used to select good incident ${}^{11}\text{Li}$ ions. The uncertainty of the incident beam intensity is $< 1\%$. The largest uncertainty in the absolute value of the cross section comes from the tracking efficiency and this is estimated to be about $\pm 10\%$.

Figure 2(a) shows the determined differential cross sections from the measurements with gas pressure equivalent to 137.4 mbar and 91.6 mbar at 0°C . The center of mass scattering angles were calculated from the scattering angles of ${}^9\text{Li}$ and the triton. The detection efficiencies are shown in the panel (b), as a function of the center of mass angle. At the 137.4 mbar, the detection efficiency drops to zero near $\theta_{cm} = 110^\circ$; this is because neither the ${}^9\text{Li}$ nor the triton ions reach the array detector near $\theta_{cm} = 110^\circ$. The efficiency of event detection near $\text{cm}=110$ was higher for the 91.6 mbar setting; under this condition, either the ${}^9\text{Li}$ ion or the triton will hit the array detector for all scattering angles.

For any particular ${}^{11}\text{Li}$ reaction event, the incident energy depends on the depth of the reaction point within the gas. In the present experiment cross sections were averaged over ${}^{11}\text{Li}$ energies from $2.8A$ to $3.2A$ MeV. The deduced differential cross sections corresponding to the two different pressure settings were consistent within experimental uncertainties. The averaged differential cross sections for transitions to the ${}^9\text{Li}$ ground state are shown in Fig. 3, where the error bars on the figure include only statistical errors. The overall uncertainty in the absolute cross section values is about $\pm 10\%$.

The transition to the first excited state ($E_x=2.69$ MeV) has been observed, and cross sections are shown also in Fig. 3. If this state were populated by a direct transfer, it would indicate that a 1^+ or 2^+ halo component is present in the ground state of ${}^{11}\text{Li}(\frac{3}{2}^-)$ because the spin-parity of the ${}^9\text{Li}$ first excited state is $\frac{1}{2}^-$. This is new information that has not yet been observed in any of previous investigations. Compound nucleus contribution should be small: at present energy, the angular distribution of compound decay must be essentially isotropic, and hence the deep minima observed in the angular distributions of the ground state and the first excited state exclude the strong contribution.

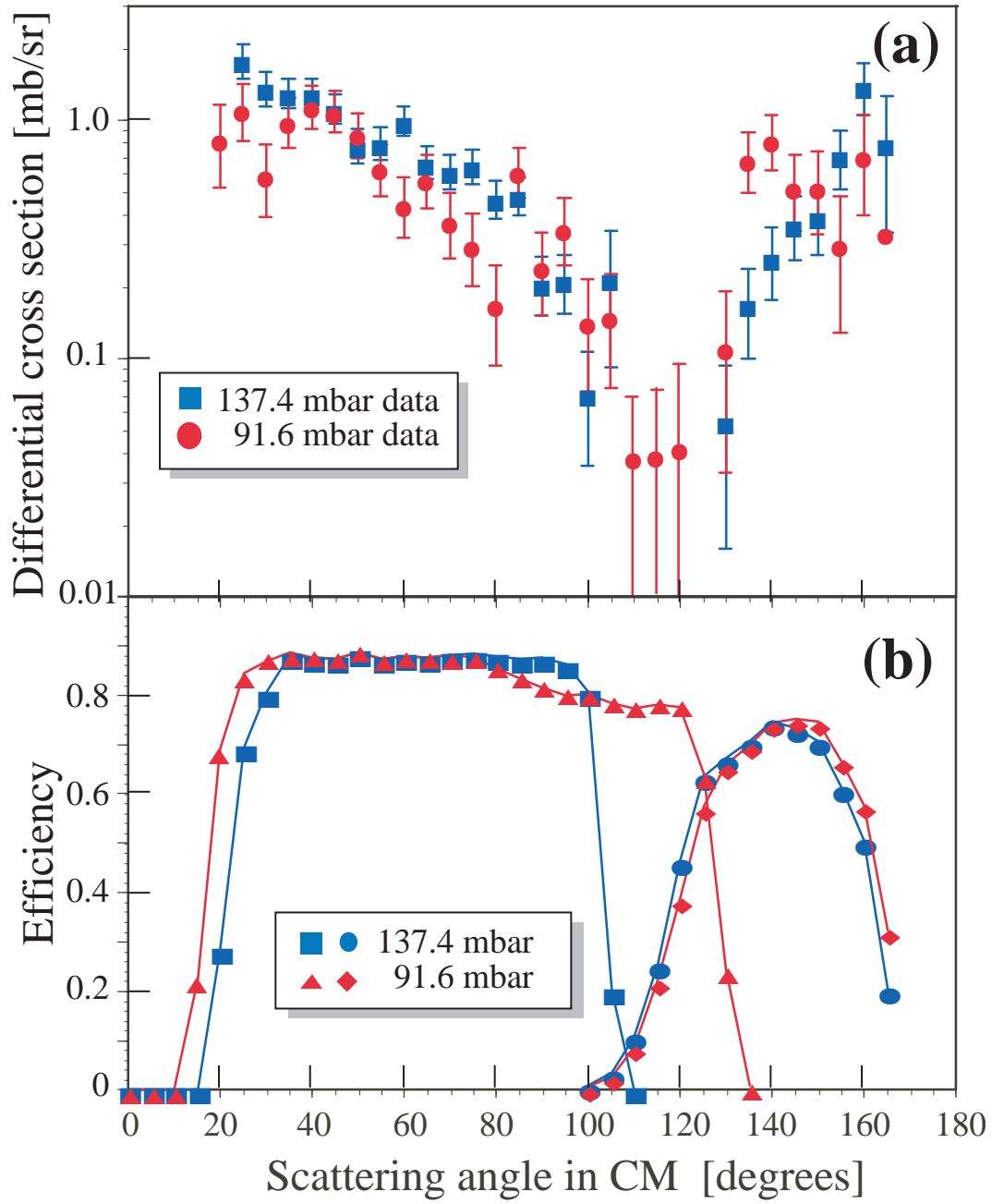


Fig. 2. (a) The comparison of the differential cross sections determined from the data sets at 137.4 mbar and 91.6 mbar. (b) The corresponding detection efficiency for each data set.

FIG. 2: (a) The comparison of the differential cross sections determined from the data sets at 137.4 mbar and 91.6 mbar. (b) The corresponding detection efficiency for each data set.

TABLE I: Optical potential parameters used for the present calculations.

	V MeV	r_V fm	a_V fm	W MeV	W_D MeV	r_W fm	a_W fm	V_{so} MeV	r_{so} fm	a_{so} fm
$p+^{11}\text{Li}$ [15]	54.06	1.17	0.75	2.37	16.87	1.32	0.82	6.2	1.01	0.75
$d+^{10}\text{Li}$ [16]	85.8	1.17	0.76	1.117	11.863	1.325	0.731	0		
$t+^9\text{Li}$ [17]	1.42	1.16	0.78	28.2	0	1.88	0.61	0		

However, before a final conclusion can be made, detailed studies of coupled channels and sequential transfer effects need to be undertaken.

Multistep transfer calculations to determine the differential cross sections to the ground state of ^9Li have been made. For these calculations several of the three-body models from Ref.[11], recalculated using the hyperspherical harmonic expansions of Ref.[12], with projection operators to remove the $0s_{1/2}$ and $0p_{3/2}$ Pauli blocked states, have been used. In particular, the P0, P2 and P3 models from [11], which have percentage $(1s_{1/2})^2$ components of 3%, 31% and 45%, respectively were used. The corresponding matter radii for ^{11}Li are 3.05, 3.39 and 3.64 fm. For comparison, a simple $(p_{1/2})^2$ model based on the P0 case, but with no n-n potential to correlate the neutrons, was also investigated. All models here do not include an excitation of ^9Li core.

The calculations reported here included the simultaneous transfer of two neutrons from ^{11}Li to ^9Li in a one step process, as well as coherently the two-step sequential transfers via ^{10}Li . The simultaneous transfers used a triton wavefunction calculated in the hyperspherical framework with the SSC(C) nucleon-nucleon force [13], and a three-body force to obtain the correct triton binding energy. The sequential transfers passed through both $\frac{1}{2}^+$ and $\frac{1}{2}^-$ neutron states of ^{10}Li , with spectroscopic factors given by respectively the s- and p-wave occupation probabilities for ^{11}Li models of [11]. The spectroscopic amplitudes for $\langle d|t \rangle$ and $\langle ^{10}\text{Li}|^{11}\text{Li} \rangle$ include a factor of $\sqrt{2}$ to describe the doubled probability when either one of the two neutrons can be transferred. S and P wave radial states were used with effective binding energies of 1.0 and 0.10 MeV respectively; this ensured a rms radii of ~ 6 fm, which is the mean n- ^9Li distance in the ^{11}Li models. The proton, deuteron and triton channel optical potentials used are shown in Table I. The differential cross sections were obtained using the FRESKO[14].

Curves in Fig. 3 show the results of the calculations. The wave function $(p_{1/2})^2$ with no n-n correlation gives very small cross sections that are far from the measured values. Also the P0 wave function, with n-n correlation but with a small $(s_{1/2})^2$ mixing amplitude, gives too small cross sections. The results of the P2 and P3 wave functions fit the forward angle data reasonably well but the fitting near the minimum of the cross section is unsatisfactory. The results may be sensitive to the choice of the optical potentials as well as the selection of the intermediate states of two-step processes. Detailed analysis of such effects should be a subject of future studies.

In summary, we have measured for the first time the differential cross sections for two-halo neutron transfer reactions of the most pronounced halo nucleus ^{11}Li . Transitions were observed to the ground and first excited state of ^9Li . Multistep transfer calculations were applied with different wave functions of ^{11}Li . It is seen that wave functions with strong mixing of p and s neutrons which includes three-body correlations, provides the best fit to the data for the magnitude of the reaction cross section. However the fitting to the angular shape is less satisfactory. The population of the first excited state of ^9Li suggests a 1^+ or 2^+ configuration of the halo neutrons. This shows that a two-nucleon transfer reaction as studied here may give a new insight in the halo structure of ^{11}Li . Further studies clearly are necessary to understand the observed cross sections as well as the correlation between the two-halo neutrons.

One of the authors, IT, acknowledges the support of TRIUMF throughout his stay at TRIUMF. The experiment is supported by GANIL and technical help from J. F. Libin, P. Gangnant, C. Spitaels, L. Olivier, and G. Lebertre are gratefully acknowledged. This work was supported by the NSERC of Canada through TRIUMF and Saint Mary's University. Part of this work was performed under the auspices of the U.S. Department of Energy by Lawrence Livermore National Laboratory under Contract DE-AC52-07NA27344. This experiment was the first experiment at the new ISAC-2 facility. The authors gratefully acknowledge R. Laxdal, M. Marchetto, M. Dombisky and all other staff members for their excellent effort for setting up the beam line and delivering the high-quality ^{11}Li beam.

* present address: RCNP, Osaka University, Mihogaoka, Ibaraki 567-0047, Japan.

† present address: Institute de Estructura de la Materia, CSIC, Serrano 113bis, E-28006 Madrid, Spain.

‡ present address: NSCL, MSU East Lansing, MI 48824-1321, USA.

[1] I. Tanihata et al., Phys. Letters B **287** (1992) 307.

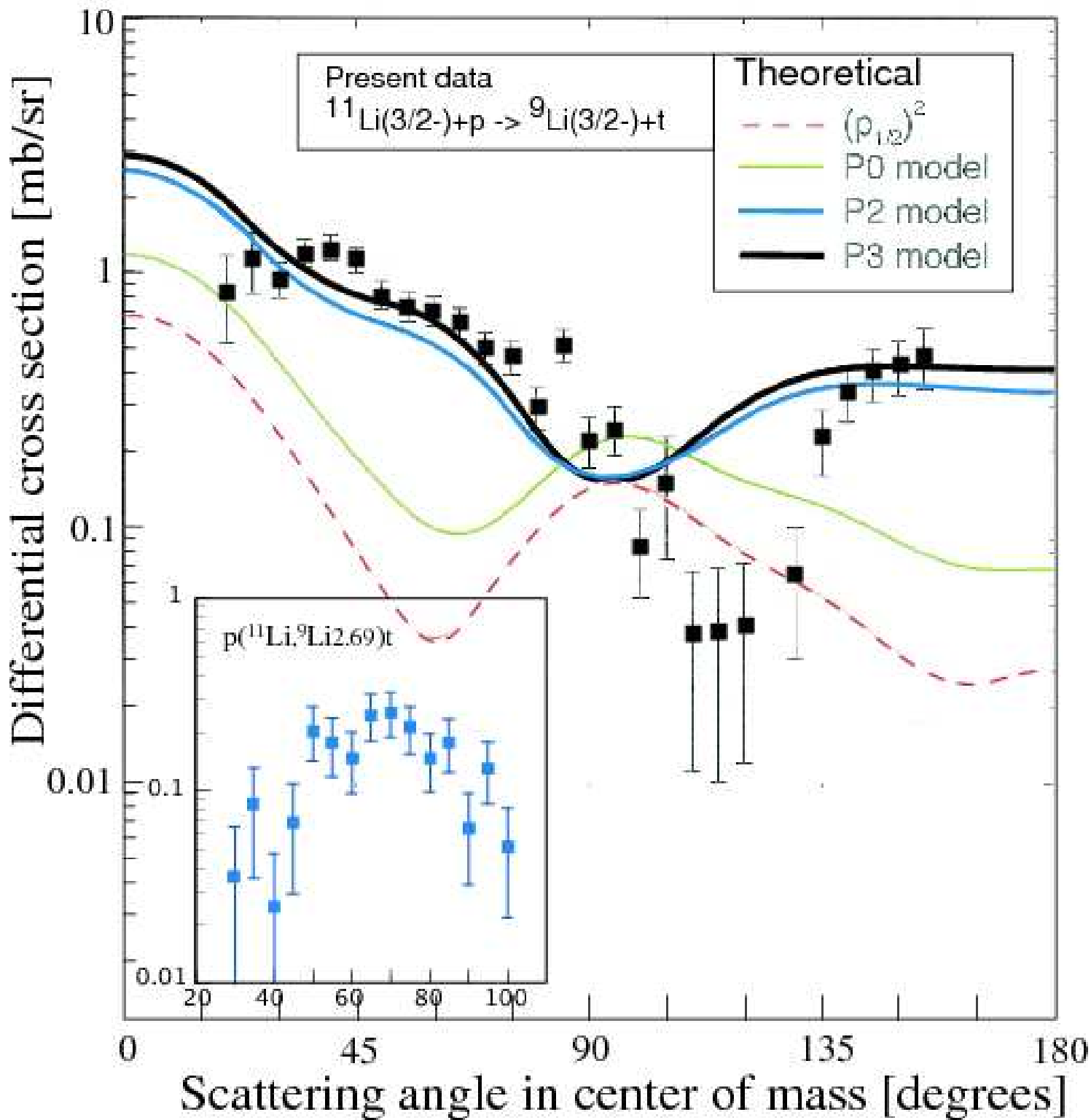


Fig. 3. Differential cross sections of (p, t) reactions to the ground state of ^9Li and to the first excited state (insert). Theoretical predictions using four different wave functions were shown by curves. See text for the difference of the curves.

FIG. 3: Differential cross sections of (p,t) reaction to the ground state of ^9Li and to the first excited state (insert). Theoretical predictions using four different wave functions were shown by curves. See text for the difference of the wave functions.

- [2] M. Zinser et al., Nucl. Phys. A **619** (1997) 151.
- [3] S. Shimoura et al., Phys. Letters B **348** (1995) 29.
- [4] T. Nakamura et al., Phys. Rev. Letters **96** (2006) 252502.
- [5] R. Sanchez et al., Phys. Rev. Letters **96** (2006) 033002.
- [6] I. Tanihata et al., Phys. Rev. Letters **55** (1985) 2676. A. Ozawa, T. Suzuki, and I. Tanihata., Nucl. Phys. A **693** (2001) 32.
- [7] L. -B Wang et al., Phys. Rev. Letters **93** (2004) 142501.
- [8] M. V. Zhukov et al., Phys. Rep. **231** (1993) 151.
- [9] Y. T. V. Oganessian et al., Phys. Rev. Letters **82** (1999) 4996.
- [10] C. E. Demonchy et al., Nuc. Instr & Methods A **573** (2007) 145.
- [11] I.J. Thompson and M.V. Zhukov, Phys. Rev. C **49** (1994) 1904.
- [12] I.J. Thompson et al., Phys. Rev. C **61**, 24318 (2000).
- [13] R. de Turreil and D.W.L. Sprung, Nucl. Phys. A **242** (1975) 445.
- [14] I. J. Thompson, Computer Physics Report **7** (1988) 167.
- [15] F. D. Becchetti and G. W. Greenless, Phys. Rev. **182** (1969) 1190.
- [16] W. W. Daehnick, J. D. Childs, and Z. Vrcelj Phys. Rev. C **21** (1980) 2253.
- [17] F.D. Becchetti and G.W. Greenless, Annual Report, J. H. Williams Laboratory, University of Minnesota (1969).